

# A Thyristor Full-Wave Rectifier With Full Control of the Conducting Angle

Ružica Stevanović

**Abstract**—A new rectifier will be described capable of control of the conducting angle in the full range from zero to  $\pi$ . A two cell ladder RC network is studied first to enable design of a phase shifter. Then a half-wave rectifier is described performing full control of the conducting angle. It incorporates a phase shifter implemented in the gate circuit of the thyristor. Using this a full wave rectifier is described and its characteristics extracted by simulation. The main advantage of the new circuit is its ability to control the conducting angle in its full range making the rectifier applicable in both electronic power supply circuits and in systems that need power control.

**Index Terms**—AC/DC converter, power supply, full-wave thyristor rectifier.

## I. INTRODUCTION

THE need for control of the conducting angle in rectifiers comes from its applications related to power control. Both, in applications where electronic circuit power supply is planned and in industrial applications, one prefers having a circuit with such capabilities. Frequently one would need a rectifier with a full scale of control of the conducting angle from 0 to  $\pi$ . We will describe here a new circuit that has these characteristics. The fundamental idea implemented is to use a two cell RC ladder network as a phase shifter controlling the firing of the thyristor's gate.

The paper is organized as follows.

## II. FULL-WAVE RECTIFYING BY A THYRISTOR

In Fig. 1 a general schematic of a full-wave controlled rectifier with thyristor is shown. The main voltage  $E$ , is rectified so that the thyristors are triggered by a control circuit which is, in this case, passive and consists of an RC ladder followed by a diac. The controlling circuitry is not shown for convenience.

Fig. 2 represent the waveforms of the main voltage and the load voltage being denoted by  $V_{out}$ . As can be seen the conducting angle  $\Theta_c$  may be less than  $\pi/2$  but generally may be controlled between 0 and  $\pi$ . During the phase angle  $\Theta_p$ , the thyristor is off.

The controlling voltage for the thyristor's gate in our solution is derived from the main voltage, attenuated, phase shifted, and, finally, brought to the thyristors gate via diac performing as a threshold element and protecting from conducting in the inverse direction. This is why we first address the phase shift circuit in the next.

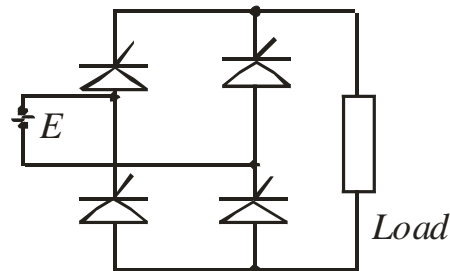


Fig. 1. Block scheme of Full-wave controlled rectifier.

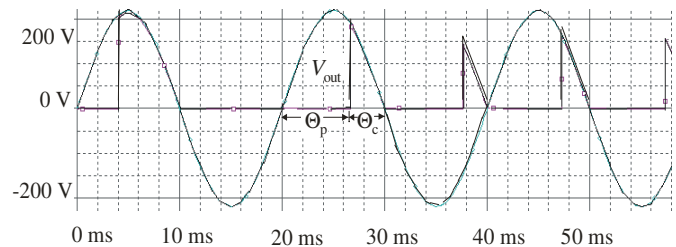


Fig. 2. Flowing angle.

## III. RC CIRCUIT AS ELEMENT OF COMPLEX CIRCUIT

The single cell passive RC circuit is known to produce a maximum phase shift of  $\pi/2$  in asymptotic conditions i.e. for infinite frequency. Having in mind that our frequency is fixed to 50 Hz very large values of the RC elements are needed even for angles near to  $\pi/2$ . Having that in mind and intending to extend the possibilities of the controlling circuit we in [3] proposed the use of two-cell passive RC ladder circuit as depicted in Fig. 3. Its frequency domain characteristics were studied in [1].

The voltage transfer function of this circuit is given with [1]

$$T(s) = \frac{V_{out}}{E} = \frac{1}{1 + s(\tau_1 + k\tau_2) + s^2\tau_1\tau_2} \quad (1)$$

where is  $\tau_1 = R_1C_1$ ,  $\tau_2=R_2C_2$ , and  $k=R_1/R_2$ . In the case  $R_1=R_2=R$  and  $C_1=C_2=C$  the poles of function (1) are  $s_1 = s_2 = -1/\tau$ , where is  $\tau=RC$ .

The phase characteristic of this function for the case when  $R_1=R_2=R$  and  $C_1=C_2=C$  is given by

$$\varphi = \text{Arg}[T(s)]\Big|_{s=j\omega} = -2 \cdot \text{arctg}(\omega RC) \quad (2)$$

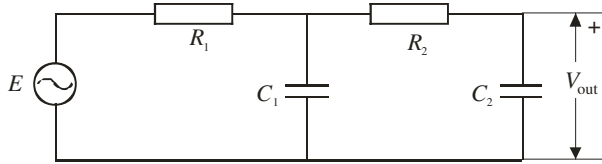


Fig. 3. Circuit of two RC sections.

As the signal frequency is fixed, the dependence of phase angle on resistance and capacitance is of interest.  $\varphi = f(R, C)$  is obtained using the programme SPICE [4]. The simulation results are shown in Fig. 4.

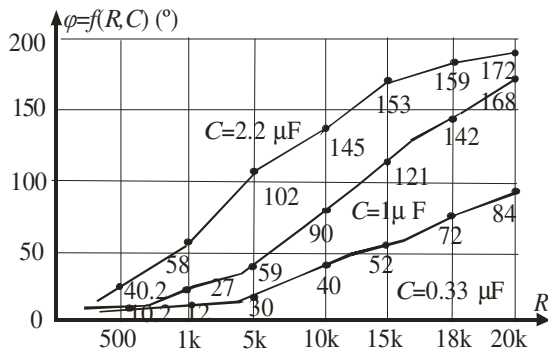


Fig. 4. Phase angle circuit with two RC sections.

Fig. 4 represents the phase angle dependence on the resistance in the RC ladder for three different values of the capacitance. By inspection of the results one may conclude first that resistances no larger than 20 kΩ are needed for the application conceived. As for the capacitances we may come out with the conclusion that  $C=1\mu\text{F}$  is practically satisfactory and, in fact, the most convenient value. Having in mind these consideration we came to the conclusion that one needs to fix the capacitance value and to use variable resistances for control of the phase angle. Note that resistors with variable resistance are easier to implement or to get from the market.

The amplitude characteristic of the function (1) in the case when  $R_1=R_2=R$  and  $C_1=C_2=C$  is obtained as

$$A = |T(s)|\Big|_{s=j\omega} = 1/\sqrt{[1+(\omega RC)^2]^2} = 1/[1+(\omega RC)^2] \quad (3)$$

or, in terms of decibells,

$$a \text{ (dB)} = 20 \cdot \log(1/A) = f(R, C). \quad (4)$$

As for the phase characteristic, using SPICE we got the dependence  $a=f(RC)$  so that we fixed the value of the capacitance and put the resistance in the role of a variable. The results are depicted in Fig. 5.

From the amplitude characteristics depicted in Fig. 5 we may come to the conclusion that even for the largest values of the resistances, if  $C = 1 \mu\text{F}$ , we get an attenuation of only about

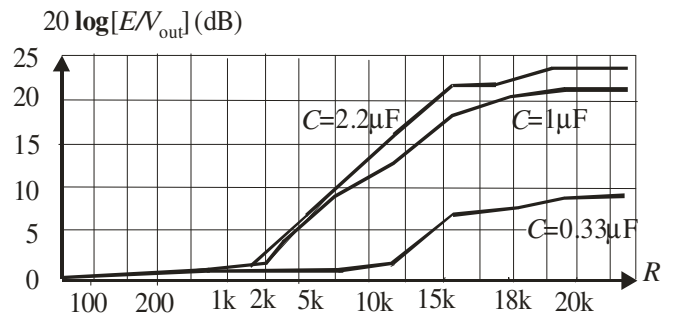


Fig. 5. Attenuation of circuit with two RC sections.

20 dB that is about ten times. This means that one may expect voltages of the order of magnitude no less than 25 V at the output of this circuit. This considerations are important for the choice of the diac that usually follows the RC ladder.

From the designers point of view, given the phase angle and the value of the capacitance  $C = 1 \mu\text{F}$ , for value of the resistance, one may use

$$R = \frac{2}{\omega C} \cdot \left[ \text{tg}(\theta_p/2) \right] \quad (5)$$

what is derived from (2). This derivation are fully approved by inspection of Fig. 4 as discussed in [3].

#### IV. HALF-WAVE THYRISTOR RECTIFIERS WITH CONDUCTION ANGLE CONTROL

The first implementation of the two-cell RC ladder in a thyristor rectifier is depicted in Fig. 6 [3]. The thyristor is triggered by the gate current pulses that are emanated from main voltage and shaped by the control circuit. The main task of the diac to generate a voltage threshold which, when is overshoted, leads the gate to conducting state. In the negative half cycle of the main voltage the DIAC and the thyristor are off.

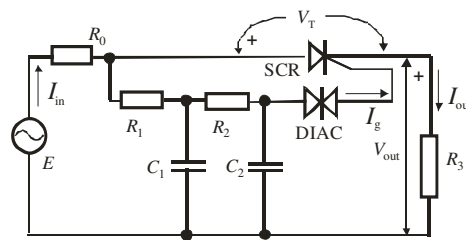


Fig. 6. Half-wave rectifier using a two-cell RC ladder.

Fig. 7. shows the transient waveform of the output voltage just after switching on the circuitry. As can be seen the phase angle is in accordance with the value that, for the given circuit parameters, may be extracted from Fig. 4. Fig. 8. depicts the current waveforms i.e. the load current ( $I_{out}$ ), the main current ( $I_{in}$ ) and thyristor's gate current ( $I_g$ ).

Finally, Fig. 9. depicts voltage waveforms for the case when  $R=20 \text{ k}\Omega$ . One may notice that conducting angles are considerably lower than  $90^\circ$ .

After exhaustive simulations, Fourier analysis of the waveforms obtained for large set of values of the resistance in the phase delay circuit, the spectra of the voltages are

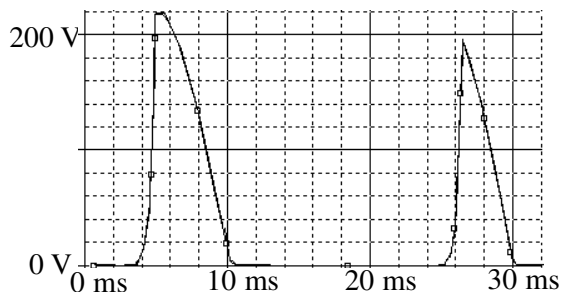


Fig. 7. Waveforms of the output voltage of the circuit of Fig. 6 (for  $R=10k\Omega$ ,  $C=1\mu F$ , and  $R_3=100\Omega$ ).

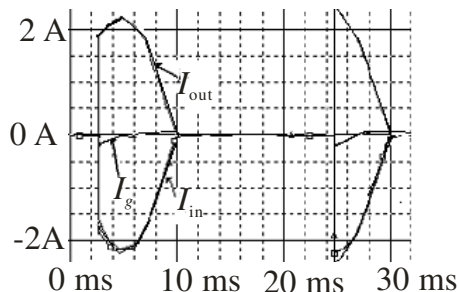


Fig. 8. Waveforms of the currents in the circuit of Fig. 6 (for  $R=10k\Omega$ ,  $C=1\mu F$ , and  $R_3=100\Omega$ ).

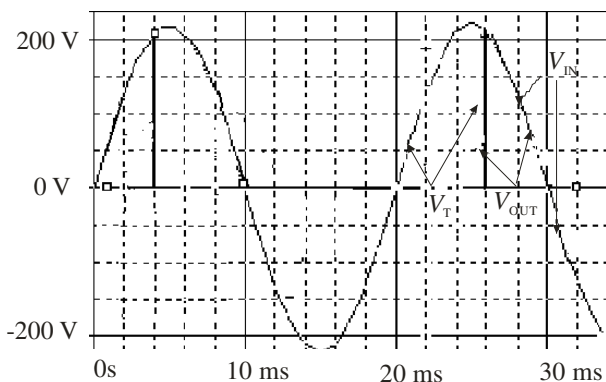


Fig. 9. Voltage waveforms (for  $R=20k\Omega$ ,  $C=1\mu F$ , and  $R_3=100\Omega$ ).

obtained. Part of these results are shown in Fig. 10 where the DC component of the output voltage is depicted as a function of the resistance in the phase delay circuit, for two values of the load resistance.

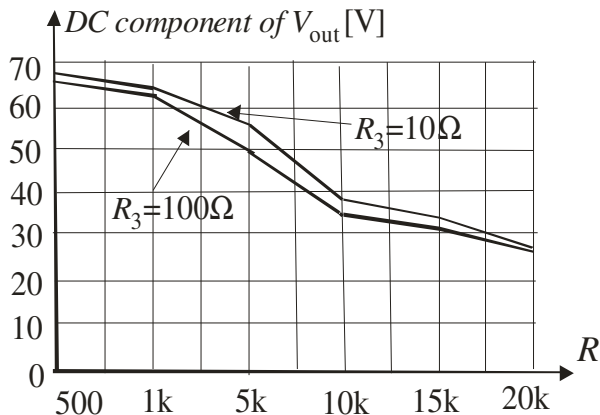


Fig. 10. Direct component of load voltage the Half-wave rectifier.

The magnitude of the first harmonic of the output voltage as a function of the resistance in the phase delay circuit for two

values of the load resistance is depicted Fig.11. As can be seen by comparing the results of Fig. 10 and Fig. 11, the alternating component of the voltage is dominant for all values of the resistance in the phase delay circuit. Nevertheless, this dominance is less persuasive for large values of resistance in the phase delay circuit.

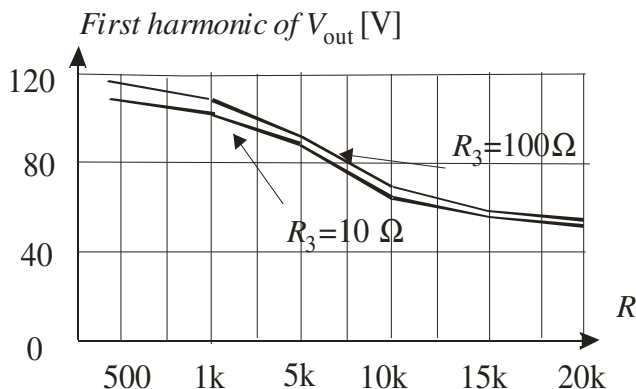


Fig. 11. The first harmonic of voltage on consumer in Half-wave rectifying.

### V. FULL-WAVE CONTROLLED RECTIFIER WITH CONTROL ANGLE OF PHASE

In order to get larger DC component in the full spectra of the obtained signal at the output full-wave rectification is needed. Application of the circuit of Fig. 6. in a full-wave rectifier is depicted in Fig. 12 and Fig. 13. Note that for simplification of the schematic we introduced a subcircuit denoted by D as shown in Fig. 12a. Fig. 12b represents a version of the full-wave rectifier in which a transformer is implemented while Fig. 13 represents a transformeless version of the rectifier. The advantages and disadvantages of these two solutions are known to the scientific public and will be not discussed here.

The full wave rectifier circuit was simulated by the SPICE program in the same manner as the half-wave circuit. The resulting simulation results are shown in the next.

In Fig. 14 the output voltage waveforms are depicted. One can notice that after transient a steady response is obtained in this case with conducting angle lower than  $\pi/2$ . In the same time one can recognize that the firing moment is in accordance with the phase angle obtained from Fig. 4.

The waveform of the output current is depicted in Fig. 15.

In the next influence of variations of the resistance in the phase shift circuit will be studied. In that sense  $R=5 k\Omega$  was chosen first. The simulation results for the output voltage are depicted in Fig. 16. Relatively large conducting angle may be observed.

Finally, a large value for the resistance in the phase shift circuit was chosen:  $R=19 k\Omega$ . The simulation results for the output voltage are shown in Fig. 17, while Fig. 18 represents the waveform of the output current. One may notice that after some transient a response is obtained with very short pulses confirming the role of the controlling circuit.

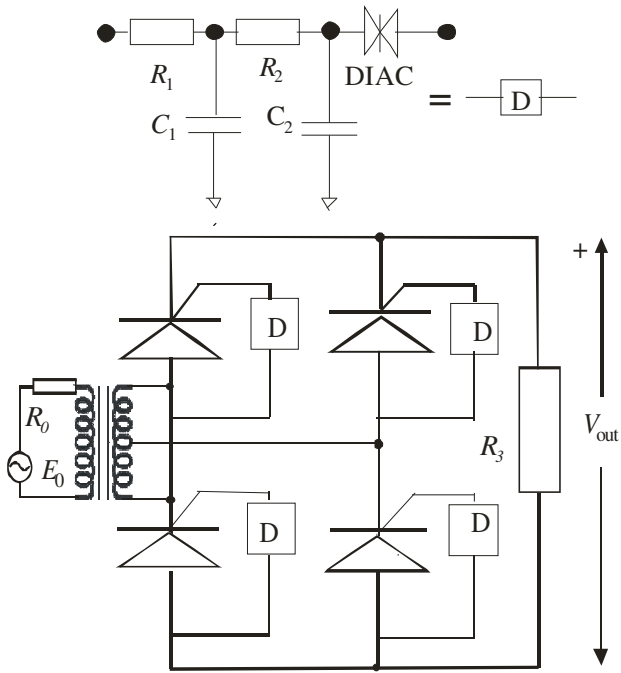


Fig. 12. (a) Symbol from the filter plus diac circuit, and (b) Full-wave controlled rectifier with transformer.

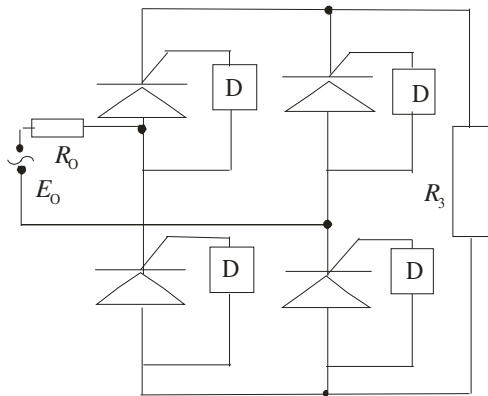


Fig. 13. Block scheme circuit for Full-wave controlled rectifier without transformer.

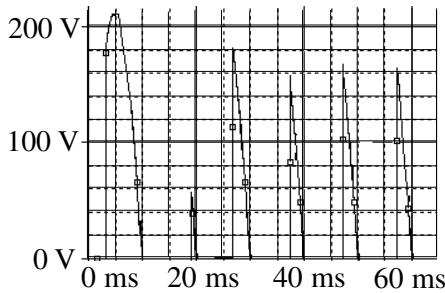


Fig. 14. Waveform of output voltage (for  $R=12\text{k}\Omega$ ,  $C=1\mu\text{F}$ , and  $R_3=100\Omega$ ).

To get a full picture of the properties of the new proposed circuit Fourier analysis of the output voltage waveform was performed for a set of resistances  $R$  and for two values of the load resistance i.e.  $R_3=10\Omega$  and  $R_3=100\Omega$ .

The results obtained after Fourier analysis are depicted in Fig. 19 and Fig. 20. The first one represents the DC component of the output voltage as a function of the resistance in the phase shift circuit. One may notice a floor of about 50V

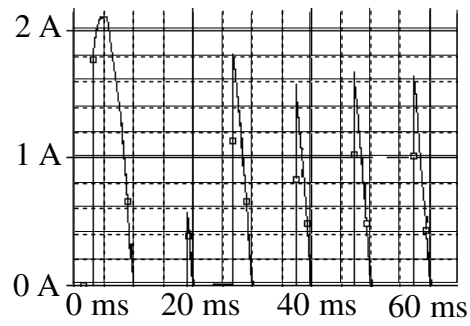


Fig. 15. Waveform of output current (for  $R=12\text{k}\Omega$ ,  $C=1\mu\text{F}$ , and  $R_3=100\Omega$ ).

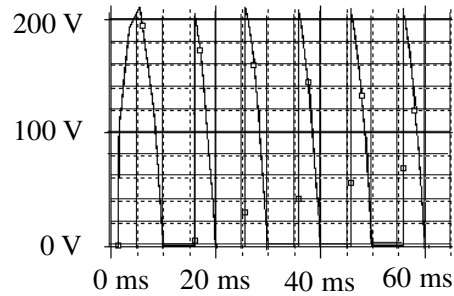


Fig. 16. Waveform of voltage (for  $R=5\text{k}\Omega$ ,  $C=1\mu\text{F}$ , and  $R_3=100\Omega$ ).

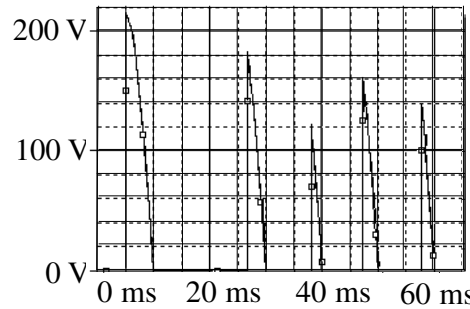


Fig. 17. Output voltage waveform (for  $R=19\text{k}\Omega$ ,  $C=1\mu\text{F}$ , and  $R_3=100\Omega$ ).

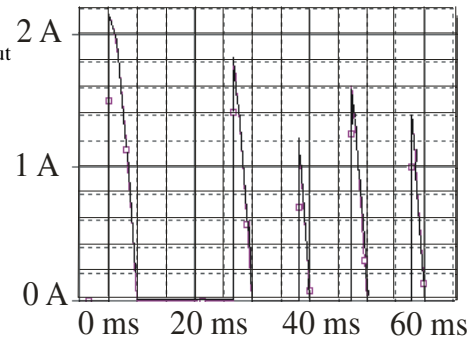


Fig. 18. Output current waveform (for  $R=19\text{k}\Omega$ ,  $C=1\mu\text{F}$ , and  $R_3=100\Omega$ ).

that is not dependent on the load resistance. On the other side, Fig. 20 depicts the dependence of the second harmonic on the resistance in the phase shift circuit. Again, as expected, for small conducting angles large harmonic compared with the DC value is obtained. Note, however, that that is the second harmonic meaning that in use of such rectifier for electronic power supply circuit easier filtering is enabled.

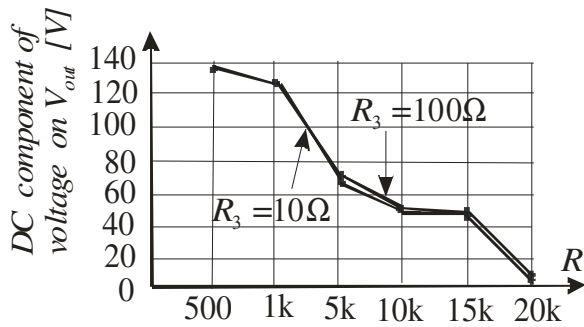


Fig. 19. DC component of output voltage of the Full-wave rectifier.

## VI. CONCLUSION

A new concept of control of the conducting angle of a thyristor rectifier was proposed and implemented in half-wave and full-wave rectification circuits. After theoretical study of the circuit and after creation of some design formulae a thorough verification procedure was implemented based on SPICE simulation of the circuits. In particular, the properties of the circuits in the frequency domain were studied in order to produce information of the applicability of the circuit in different applications.

It is our opinion that the concept proposed is promising and we expect in the future to get further improvement by introducing voltage controlled resistors so enabling phase angle control by single controlling signal.

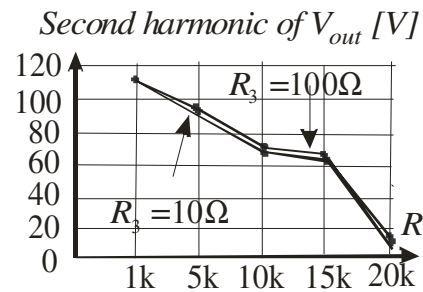


Fig. 20. The second harmonic of voltage on load.

## REFERENCES

- [1] Litovski, V. „Basics of Electronics“, Akademska misao, Belgrade, 2006, in serbian.
- [2] Dokić, B. „Power electronics –converters and regulators“, ETF Banja Luka, 2000, in serbian.
- [3] Stevanović, R. „Thyristor rectification with conducting angles less than 90 degrees“, Tehnika, Belgrade, No. 4, 2008, accepted for publication, in serbian.
- [4] Banzaf, W., „Computer-Aided Circuit analysis using SPICE“, Prentice Hall, Englewood Cliffs, N. J., 1989.
- [5] Taylor, P.D., „Thyristor design and realization“, John Wiley and Sons, Chichester, 1987.